PROCEEDINGS OF
INTERNATIONAL CONFERENCE ON NEW TRENDS IN APPLIED SCIENCES
https://proceedings.icontas.org/
International Conference on New Trends in Applied Sciences (ICONTAS'23), Konya, December 1-3, 2023.

AN EFFICIENT FEATURE ANALYSIS METHOD OF BIOLOGICAL DATA FOR IMPROVING CATTLE CONCEPTION RATE

Tatsuya Komatsu, Hiroto Noma, Takumi Asaoka, Hidetoshi Oya
Tokyo City University
0009-0008-1110-1217, 0009-0007-0972-8857, 0009-0002-5890-5470, 0000-0003-1046-5832
g2281424@tcu.ac.jp, g2381449@tcu.ac.jp, g2281401@tcu.ac.jp, hide@tcu.ac.jp

Ryotaro Miura
Nippon Veterinary and Life Science University, 0000-0002-4945-0649
ryotaro.miura@nvlu.ac.jp

Koji Yoshioka
Azabu University, 0000-0003-1600-7955
k-yoshioka@azabu-u.ac.jp

ABSTRACT: In this paper, we show an efficient feature analysis method of body surface temperature (ST) data so as to develop accurate prediction systems for artificial insemination (AI) timing of cattle. In the proposed analysis method, by using the fundamental waveform synthesis method based on the Fourier transform, approximate waveforms for the target waveform were derived. Additionally, reconstructed waveforms which does not correspond to both high frequency noise and circadian rhythm were generated. The two reconstructed waveforms derived from the approximate waveforms were used to predict the optimal AI timing and to discriminate the normal phase, respectively.

Key words: cattle, artificial insemination (AI), ventral tail base surface temperature, prediction system

INTRODUCTION

It is well known that estrus detection plays a very important role for improving reproductive performance of the dairy herd and beef cattle industries. Farmers estimate the optimal artificial insemination (AI) timing, which occurs before ovulation, by detecting estrus. For estrus, failure of detection or misdiagnosis leads to missed or untimely AI, and these results cause economic losses. The loss for missing out on optimal AI timing becomes approximately $18 per a cow per day for milk and $11 per cow per day for feed. Thus, detection of estrus in cattle is very important for predicting optimal AI timing. Although estrus detection based on visual observation of behavioral signs (i.e. standing events) by specialists, 40% of estrus is missed out [López-Gatius (2012)]. It is known that the duration of estrous cycle is 21 days. In the case of farmer with 125 cows, missing 40% of the estrus causes the farmer to lose approximately $11,822 per cycle. It is obvious that farmers improving reproductive efficiency (i.e. detecting when cattle are in estrus and inseminating them accurately) can reduce loss of time and costs. Therefore, various detection methods for estrus/optimal AI timing in cattle have been developed [Schweinzer et al. (2019), Sakatani et al. (2016), Nogami et al. (2014)]. The detection methods based on monitoring ventral tail base surface temperature (ST) for estrus has also been presented which sensors are less expensive for farmers and less stressful for cattle than sensors of vaginal temperature [Miura et al. (2017)]. In the work of Miura et al., it has also been shown that ST in pre-ovulatory period shows variations clearly. i.e. ST decreases about 2 days before ovulation “trend B”, and it increase about 1 day before ovulation “trend A”. Especially, trend A was reported to change ST to a greater degree than trend B. Such variations are occurred by hormonal changes in the cattle. Based on these fluctuations caused by estrus, prediction method of optimal AI timing by monitoring ST is developed [Matsumoto et al. (2022)].

From the above discussions, we show an efficient feature analysis method of data (ST) to develop accurate prediction systems for AI timing of cattle. In the proposed analysis method, by using the fundamental waveform synthesis method based on the Fourier transform, approximate waveforms for the target waveform (ST) are derived. Because of this, frequency elements consisting of the target waveform can be obtained. One can easily see that frequency elements mean “fundamental” and “harmonic”, and “harmonic (M)” is appropriately selected

to generate accurate approximate waveforms. The reconstructed waveforms were calculated by using the frequency elements which don't correspond to the high-frequency noise (*M=30*) and circadian rhythms (*M=20*) respectively. Moreover, for reconstructed waveform with *M=30*, scalograms obtained by applying the continuous wavelet transform are calculated, and NSI^{α} (Normalized Spectrum Index with degree α) can be generated by using scalograms. Based on NSI^{α}, the peaks related to the effect of estrus can be detected.
For reconstructed waveform with *M=20*, discrimination of normal phase was performed by extracting the maximum and minimum values. Note that "the normal phase" is defined as the period which does not corresponds to ovulation in this study. We see from analysis results for the reconstructed waveform that features for variations of ST before ovulation can efficiently captured, i.e. efficient features correspond to ovulation can be extracted. In this paper, by using the proposed analysis method, we show analysis results for biological data.

MATERIALS AND METHODS

ST data

Nine female cows (five Holstein Friesian heifers, one Japanese Black heifer, and three Japanese Black cows, 2.7 ± 0.8 years old: mean ±SD) with normal estrous cycles were used in summer (August–September), autumn (October–November) and winter (January-–February; three animals per season). A wireless sensor were attached to the lower surface of the ventral tail base. Examples of measured ST are shown in Figures 1 and 2. In these figures, the horizontal axis indicates the number of days until ovulation [day] and the vertical one indicates ST [°C]. The actual day of ovulation is set as 0 [day] and the sampling rate is 120 [s]. The "No." means to the individual identification number.

Fundamental Waveform Synthesis

We apply the fundamental waveform synthesis on Fourier series expansion [Yamaguchi et al. (2008)] to the ST data and then approximate waveforms are generated. Now we assume that the preprocessed-waveform can be expressed in the form of a Fourier series expansion. It is well known that Fourier series expansion for periodic signal $f(t)$ is given by

$$f(t) = \frac{a_0}{2} + \sum_{n=1}^{\infty} a_n \cos\left(\frac{2\pi nt}{T}\right) + \sum_{n=1}^{\infty} b_n \sin\left(\frac{2\pi nt}{T}\right), \tag{1}$$

where T is the fundamental period (i.e. T^{-1} is the fundamental frequency), and M is a parameter which represents the order of the harmonics. Moreover, a_0, a_n and b_n are the Fourier coefficients. In this paper on the basis of the Fourier series expansion, we suppose that the approximate waveform $\hat{f}(\mathrm{t})$ is described as

$$\hat{f}(t) = \frac{\alpha_0}{2} + \sum_{n=1}^{M} \alpha_n \cos\left(\frac{2\pi nt}{T}\right) + \sum_{n=1}^{M} \beta_n \sin\left(\frac{2\pi nt}{T}\right). \tag{2}$$

In (2), α_0, α_n and β_n are the Fourier coefficients of the approximate waveform. In this paper, the Fourier coefficients of the approximate waveform are searched by using the steepest descent method. The coefficients α_0, α_n and $\beta_n$are determined by using mean square error (MSE). Note that the stopping condition is $\mathrm{MSE} < 10^{-4}$. In this paper, the parameter M in (2) is selected as $M = 500$. Note that, the sampling interval is temporarily set at 0.01[s], i.e., the fundamental frequency is assumed to be 0.005[Hz]. Figure 3 shows the ST waveform shown as the blue line and approximate waveform described as red line.

Reconstruction of Approximate Waveform

The approximate waveforms were reconstructed by using only specified frequency components. In this paper, we set *M* as the following two values:

(i) *M=30*: Reconstructed waveform with components in the frequency band corresponding to the high frequency noise removed.
(ii) *M=20*: Reconstructed waveform with components in the frequency bands corresponding to circadian rhythms (temperature changes in approximately 24-hour cycles due to cattle's life rhythm) removed in addition to the high frequency noise.

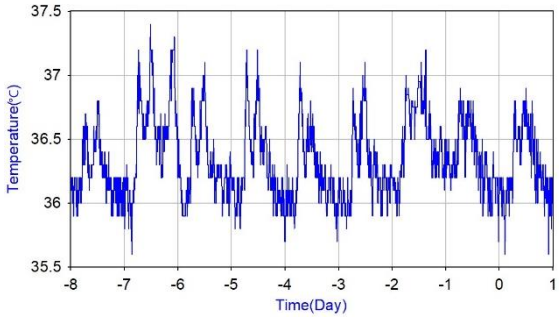

Figure 1. Raw Data (No.64 Autumn)

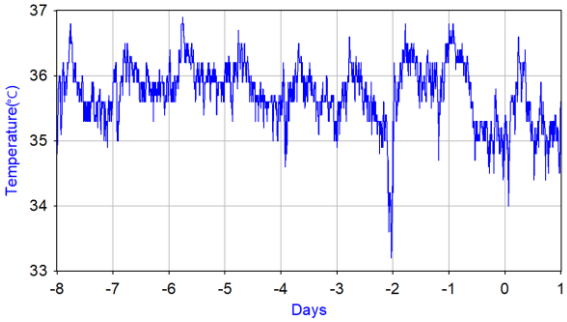

Figure 2. Raw Data (No.70 Winter)

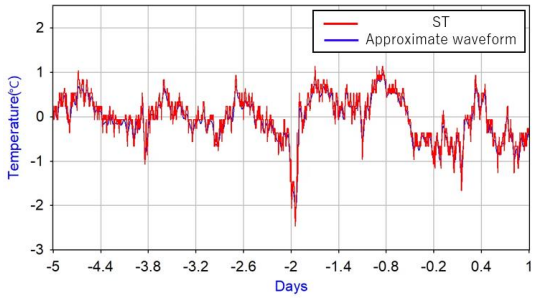

Figure 3. ST and Approximate Waveform

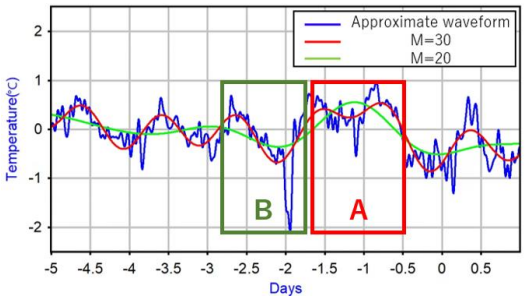

Figure 4. Approximation Waveform and Reconstructed Waveforms(*M = 30, 20*) for Figure 3

Figure 4 shows the approximate waveform and the reconstructed waveforms with *M=30* and *M=20* respectively. The reconstructed waveform with *M=30* shows the characteristics of circadian rhythms. Moreover one can see that fluctuations corresponding to noises are suppressed. The reconstructed waveform with *M=20* represents gradual transitions in which the circadian rhythm has been eliminated. In addition, ST decreased approximately 3 days before ovulation and increased 1.5 days before ovulation. These changes in the reconstructed waveform are similar to the characteristic of ST fluctuations before ovulation shown in the literature [Miura et al. (2017)]. Figure 4 shows that the trends A and B before ovulation has been captured. The reconstructed waveforms shown in Figure 4 were generated by using the data of the entire ovulation cycle, but when predicting the actual day of ovulation, it is necessary to estimate it based on the data received from the sensors in real time. In other words, it is necessary to generate reconstructed waveforms sequentially from the data measured from time to time and to capture calculating fature parameters related to ovulation. Therefore, an approximate waveforms are generated every time one hour's of data has been accumulated.

Prediction of Optimal AI Timing

Suppression of Circadian Rhythm Processing

The reconstructed waveform (*M=30*) is analyzed by suppressing the circadian rhythm to extract the characteristic of emperature fluctuations prior to ovulation. One can easily see that the circadian rhythm may interfere with analysis. In order to remove the influence of the circadian rhythm, we suppress the fluctuation of circadian rhythm from reconstructed waveform (actual value of reconstructed waveform − mean value of reconstructed waveform for the same hour on the previous 2 days and current time). $x^*(k)$ is given as:

$$x^\star(k) = x(k) - \frac{1}{3}\{x(k-2) + x(k-1) + x(k)\} \tag{3}$$

where $x(k)$ denote ST at time *k* and *k* is a sample number. Figure 6 shows $x^*(k)$ obtained from the waveform in Figure 5.

Time Frequency Analysis Methods

The time frequency analysis methods (continuous wavelet transform and NSI$^{\alpha}$ [Matsumoto (2022)]) are adopted in order to detect pre-ovulatory ST fluctuation from the preprocessed waveform. Figures 7 and 8 show the results of applying the wavelet transform and NSI$^{\alpha}$ to Figure 6, respectively. The scalograms shown in Figure 7 is output of the wavelet transform and is a three-dimensional graph with time on the horizontal axis, frequency on the vertical one, and energy intensity. The energy intensity is shown as color map from blue to red. NSI$^{\alpha}$ (Normalized Spectrum Index α) is adopted to convert the scalogram to two dimensional waveform. Note

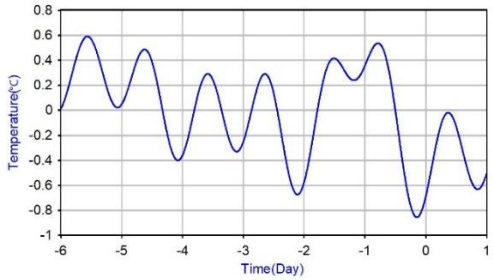

Figure 5. Reconstructed Waveform (*M = 30*) for Figure 2

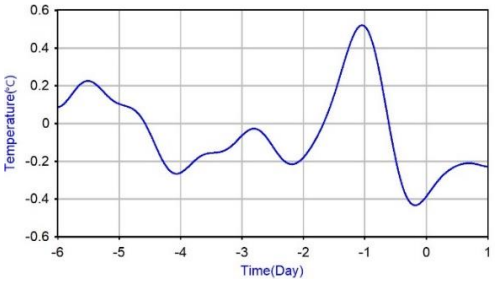

Figure 6. After Circadian Rhythm Suppression.

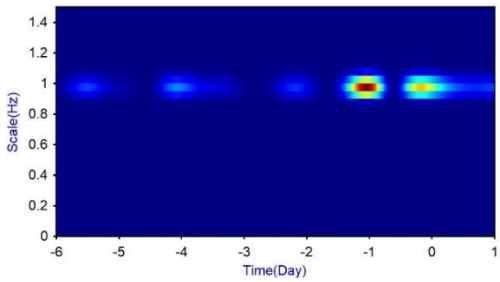

Figure 7. An Example of Scalograms

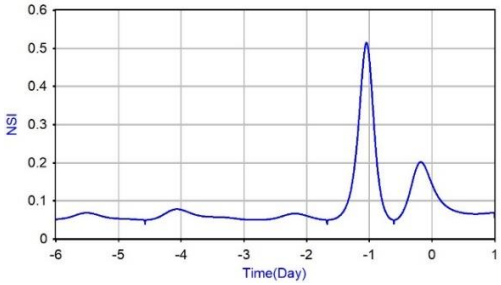

Figure 8. An Example of NSI$^{\alpha}$

that NSI$^{\alpha}$ is considered as center of gravity in scalograms. In this study we set the weighting parameter α=2.0. NSI$^{\alpha}$ has been able to capture features for characteristic variation of ST before ovulation. One can see from Figure 8 that NSI$^{\alpha}$ takes maximum value at approximately -1[d] and the peak corresponds to trend A.

Peak Detection mehod

The peak detection method is based on the time when the difference between the maximum value of the interval of the latest data for one day and the latest data in the reconstructed waveforms generated from time to time is greater than the threshold value *th = 0.25*. In addition, a decreasing trend in the reconstructed waveform at the time of peak occurrence in NSI$^{\alpha}$ gives a criterion. In other words, due to the fact that the reconstructed waveform after the rise shows in a decreasing trend after the peak.

Discrimination of Normal Phase

Feature Extraction

Figure 9 represents the reconstructed waveforms which are generated by each time one hour of accumulated data. We see from Figure 9 that for the reconstructed waveform (*M=20*) that the circadian rhythm is suppressed. In Figure 9, ST fluctuations tend to be larger than normal before -3 [day], which may be due to the continuous occurrences of trend B and trend A. These trends represent fluctuations attributable to the ovulation. Therefore, we focused on the transition of the maximum and median values of the extended reconstructed waveforms. The maximum and median values of the latest daily interval of the reconstructed waveform are shown in Figure 10. The maximum and median values increase from about 2[day] before ovulation with the occurrence of trend A. Moreover the maximum and median values for each 8-hour period are searched respectively, and linearly interpolated waveform $max_8(k)$ and $median_8$(k) are shown in Figure 11. In this study, a status waveform (see Figure 12) is derived to visualise the state in which the maximum value and median value tends to increase defined as follows:

$$St(t) = \begin{cases} 1 & (\max_8(\mathrm{t}) < \max_8(\mathrm{t}+1)) \wedge \mathrm{median}_8(\mathrm{t}) < \mathrm{median}_8(\mathrm{t}+1)) \\ 0 & (otherwise). \end{cases} \quad (3)$$

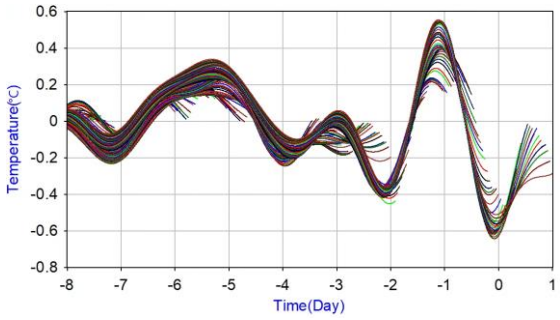

Figure 9. Reconstructed Waveform (*M=20*) for Figure 2

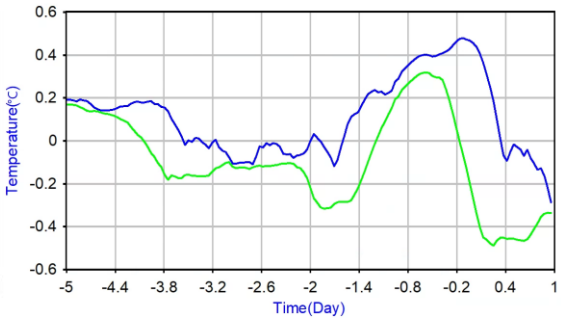

Figure 10. Maximum and Median Values

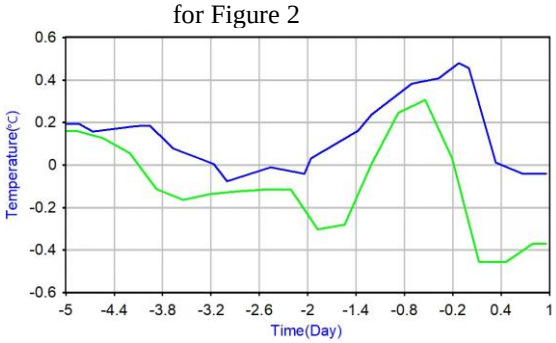

Figure 11. $max_8(k)$ and min_8(k) Waveforms

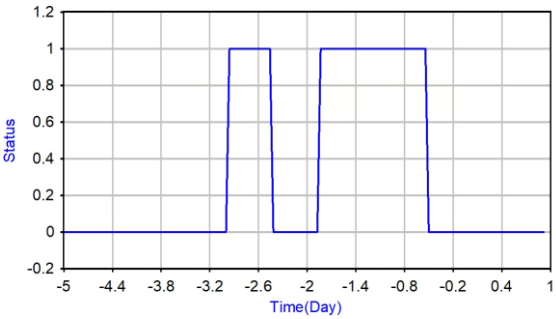

Figure 12. Status Waveform

RESULTS AND FINDINGS

In the normal phase discrimination, the time in *St(t)=1*, was determined as the possible phase of optimal AI timing. In other words, the periods between *St(t)=0* means the normal phase. Based on this criterion, following algorithm for predicting optimal AI timing is developed:

(i) Calculate the reconstructed waveforms with *M=20* and *30* respectively.

(ii) Derive a status waveform from the reconstructed waveform (*M=20*).

(iii) Search for *St(t)=1* in status waveform, and if it is not detected, then return to step (i).

(iv) Perform the detection method of optimal AI timing. In the case that the peak of NSI^{α} was detected, the detection time is judged as optimal AI timing. If not, return to step (i).

Table 1 shows the time of occurrence of the *St(t)=1* closest to the peak of NSI^{α} was detected and predicted time of optimal AI timing. This is because a large increase was detected due to the occurrence of ST fluctuations related to ovulation, allowing discrimination between normal and ovulatory phase (around -2 days). In the No. 70 Autumn data, the peaks of NSI^{α} were detected at -2.1 and -1.04 [day], but the optimal AI timing could be identified as -1.04 [day] by normal phase discrimination. In addition, the detection 1.5 days before ovulation also makes it possible to prepare AI in advance. In previous study [Sumiyoshi, Tanaka and Kamomae (2020)] significantly higher conception rates have been reported when AI is performed approximately 0-24 [h] before ovulation. For multiparous cows, the conception rate was as high as 78.0% in the time range of 6-18 hours prior to ovulation. It has also been reported that the conception rate for AI performed 0-24 hours prior to insemination was approximately 57.6%, which is higher than the conception rate for all cows (47.0%) [Sumiyoshi, Tanaka and Kamomae (2020)]. Based on these results, the optimal insemination phase was set at 0-24 [h] and the effective phase at 6-18 [h] in this study. From above discussion, in the case that AI was performed 0.5[day] after the detection time, 7 out of 9 data were in the effective phase and 4 data indicated optimal phase of AI. In the data where detection failed, it is possible that this was because no significant ST increase was detected. Although accurate prediction of the optimal timing of AI was achieved, the time of normal phase discrimination varied from -2.66 to -1.50. Such failures are caused by large variations of ST during the normal phase, i.e., and individual differences in the occurrence time of pre-ovulatory ST fluctuations.

Table 1. Peak Detection Time and Time when *St(t)=1*

ID	64 autumn	70 autumn	70 winter	71 summer	3957 summer
Time when *St(t)=1* [day]	-1.66	-1.50	-1.83	-1.95	-1.62
Peak Detection Time[day]	−0.87	-1.04	-1.2	-0.75	-0.45
ID	5779 summer	5779 autumn	5779 winter	9213 winter	
Time when *St(t)=1* [day]	-1.50	-1.50	-2.50	-2.66	
Peak Detection Time[day]	-2.16	-0.95	-0.62	-2.20	

CONCLUSION

In this paper, we have proposed analsys methods based on fundamental waveform synthesis method. The two reconstructed waveforms derived from the approximate waveforms were used to predict the optimal AI timing and to discriminate the normal phase, respectively. In the analysis in prediction of optimal AI timing, scalograms based on continuous wavelet transform are firstly generated, and next $\boldsymbol{NSI^{\alpha}(k)}$ is obtained by using scalograms. There are distinctive features (abrupt peaks) in the $\boldsymbol{NSI^{\alpha}(k)}$. Namely, if characteristics for such features can be detected, then it means the time is considered as optimal AI timing. However, these peaks of $\boldsymbol{NSI^{\alpha}}$ could occur 2[day] before ovulation. The short coming of the prediction method of optimal AI timing was handled by improving the discrimination method of the normal phase. When both the maximum and median values of the reconstructed waveform didn't show an upward trend, the normal phase was judged was determined for the other periods. However, the time of occurrence of the *St(t)=1* closest to the peak of $\boldsymbol{NSI^{\alpha}}$ within the period -2.66 to -1.50[day], results in a large variation between individuals. One of future tasks is an extension to the prediction system embedding pattern recognition methods.

FUNDINGS

This work was supported by A-STEP (Adaptable and Seamless Technology Transfer Program through Target driven R&D. Grant Number: JPMJTM22BM).

REFERENCES

López-Gatius, F. (2012). *Factors of a noninfectious nature affecting fertility after artificial insemination in lactating dairy cows. A review*. Theriogenology, 77, 1029.E041.

Matsumoto, K., Komatsu, T., Miura, R., Oya, H., Hoshi, Y. (2022). *Analysis of body surface temperature data based on wavelet transform for detection of optimal insemination phase in cattle.* In: 2022 25th International Conference on Mechatronics Technology (ICMT), Kaohsiung, Taiwan, pp. 1–6.

Miura, R., Yoshioka, K., Miyamoto, T., Nogami, H., Okada, H., Itoh, Y. (2017). *Estrous detection by monitoring ventral tail base surface temperature using a wearable wireless sensor in cattle.* Animal Reproduction Science, 180, 50-57.

Nogami, H., Okada, H., Miyamoto, T., Maeda, R., Itoh, T. (2014). *Wearable wireless temperature sensor nodes appressed to the base of a calf's tail.* Sens. Mater., 26, 539.E45.

Roelofs, J., Lopez-Gatius, F., Hunter, R., Van Eerdenburg, F., Hanzen, C. (2010). *When is a cow in estrus? Clinical and practical aspects.* Theriogenology, 74, 327-344.

Sakatani, M., Takahashi, M., Takenouchi, N. (2016). *The efficiency of vaginal temperature measurement for detection of estrus in Japanese Black cows.* J. Reprod. Dev., 62, 201.E07.

Schweinzer, V., Gusterer, E., Kanz, P., Krieger, S., Suss, D., Lidauer, L., Berger, A., Kickinger, F., Ohlschuster, M., Auer, W., Drillich, M., Iwersen, M. (2019). *Evaluation of an ear-attached accelerometer for detecting estrus events in indoor housed dairy cows.* Theriogenology, 130, 19.E5.

Sumiyoshi, T., Tanaka, T., Kamomae, H., (2020). *An investigation of the time period within which frozen-thawed semen delivers a high conception rate in lactating dairy cows.* Journal of Reproduction and Development 66, 277–280.

Suthar, V.S., Burfeind, O., Bonk, S., Dhami, A.J., Heuwieser, W. (2012). *Endogenous and exogenous progesterone influence body temperature in dairy cows.* J. Dairy Sci., 95, 2381.E389.

Yamaguchi, Y., Shimazaki, S., Hagino, K., Oya, H., Kirioka, S., Okai, T. (2008). *Development of an early recognition system for extracted waveforms based on ECG analysis during cardiopulmonary resuscitation.* Research Report on Science and Technology for Fire Fighting and Disaster Prevention in 2006, pp. 37-51. (In Japanese)